

Discovery of 4-(5-(Cyclopropylcarbamoyl)-2-methylphenylamino)-5-methyl-*N*-propylpyrrolo[1,2-*f*][1,2,4]triazine-6-carboxamide (BMS-582949), a Clinical p38 α MAP Kinase Inhibitor for the Treatment of Inflammatory Diseases[†]

Chunjian Liu,* James Lin, Stephen T. Wroblewski, Shuqun Lin, John Hynes, Jr., Hong Wu, Alaric J. Dyckman, Tianle Li, John Wityak, Kathleen M. Gillooly, Sidney Pitt, Ding Ren Shen, Rosemary F. Zhang, Kim W. McIntyre, Luisa Salter-Cid, David J. Shuster, Hongjian Zhang, Punit H. Marathe, Arthur M. Doweiko, John S. Sack, Susan E. Kiefer, Kevin F. Kish, John A. Newitt, Murray McKinnon, John H. Dodd, Joel C. Barrish, Gary L. Schieven, and Katerina Leftheris

Bristol-Myers Squibb Research and Development, P.O. Box 4000, Princeton, New Jersey 08543-4000

Received May 4, 2010

The discovery and characterization of **7k** (BMS-582949), a highly selective p38 α MAP kinase inhibitor that is currently in phase II clinical trials for the treatment of rheumatoid arthritis, is described. A key to the discovery was the rational substitution of *N*-cyclopropyl for *N*-methoxy in **1a**, a previously reported clinical candidate p38 α inhibitor. Unlike alkyl and other cycloalkyls, the sp² character of the cyclopropyl group can confer improved H-bonding characteristics to the directly substituted amide NH. Inhibitor **7k** is slightly less active than **1a** in the p38 α enzymatic assay but displays a superior pharmacokinetic profile and, as such, was more effective in both the acute murine model of inflammation and pseudoestablished rat AA model. The binding mode of **7k** with p38 α was confirmed by X-ray crystallographic analysis.

Introduction

The identification and development of inhibitors of p38 α mitogen-activated protein (MAP^a) kinase as orally active therapeutic agents for the treatment of inflammatory diseases has been one of the most active research areas in drug discovery for the past decade. Because p38 α MAP kinase plays a critical role in regulating the biosynthesis of many inflammatory cytokines, including tumor necrosis factor alpha (TNF- α) and interleukin-1 β (IL-1 β), p38 α inhibitors have been considered a promising solution for the treatment of inflammatory diseases.¹ Numerous preclinical studies² have demonstrated that inhibition of p38 α MAP kinase can effectively inhibit TNF- α production both in vitro and in vivo. Excessive production of TNF- α and IL-1 β is believed to underlie many inflammatory diseases.³ Blockage of TNF- α function by biological agents such as etanercept, a soluble TNF- α receptor, and infliximab, a TNF- α antibody, has proven effective in the treatment of rheumatoid arthritis and other autoimmune diseases.⁴ A number of reviews covering the progress in this area have been published.⁵ Despite a number of compounds having advanced into clinical trials, including VX-702,^{6,7} Pamapimod,^{7,8} BIRB-796,⁹ Scio-469,^{7,10} and PH-797804 (aS)¹¹ (Figure 1), proof of concept for the efficacy and safety of a p38 α inhibitor has yet to be realized.⁷

[†]PDB deposition number: 3MVL.

*To whom correspondence should be addressed. Phone: 609-252-3682. Fax: 609-252-7410. E-mail: chunjian.liu@bms.com.

^aAbbreviations: MAP, mitogen-activated protein; TNF- α , tumor necrosis factor alpha; IL-1 β , interleukin-1 beta; hPBMC, human peripheral blood mononuclear cells; LPS, lipopolysaccharide; AA, adjuvant arthritis; HHA, human hepatotoxicity assay; hERG, human ether-a-go-go-related gene.

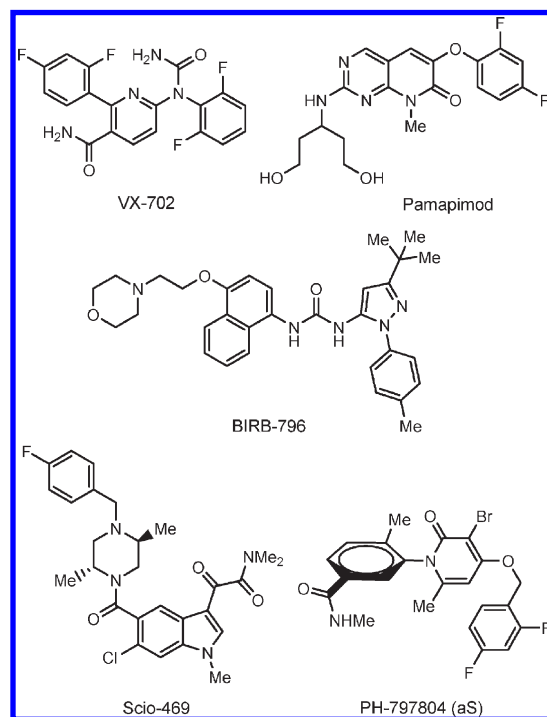


Figure 1. Examples of reported clinical p38 α MAP kinase inhibitors.

A recent paper from our group has disclosed pyrrolo[2,1-*f*][1,2,4]triazine derivatives **1a** and **1b** (Figure 2) as potent p38 α MAP kinase inhibitors for consideration as clinical candidates.¹² However, compounds **1a** and **1b** suffered from high clearance in vivo, which resulted in low exposures in

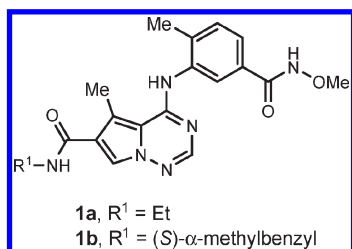


Figure 2. Our previously disclosed p38α MAP kinase inhibitors **1a** and **1b**.

animals. Subsequent studies revealed that **1a** was rapidly converted to the corresponding carboxylic acid as the major metabolite from the hydrolysis of *N*-methoxybenzamide. Naturally, efforts to modify **1a** and **1b** were focused on eliminating the presence of the problematic *N*-methoxybenzamide. In our previous disclosures,^{12,13} it was shown that the *N*-methoxybenzamide functionality in **1a** and **1b** could be replaced with urea, carbamate, and reverse amide moieties not containing the methoxylamino group, resulting in a number of highly potent p38α MAP kinase inhibitors. Herein, we describe an alternative approach to directly replace the *N*-methoxy group that ultimately led to a superior p38α inhibitor, with overall properties appropriate for clinical development, which is currently in phase II clinical trials for the treatment of rheumatoid arthritis.

Chemistry

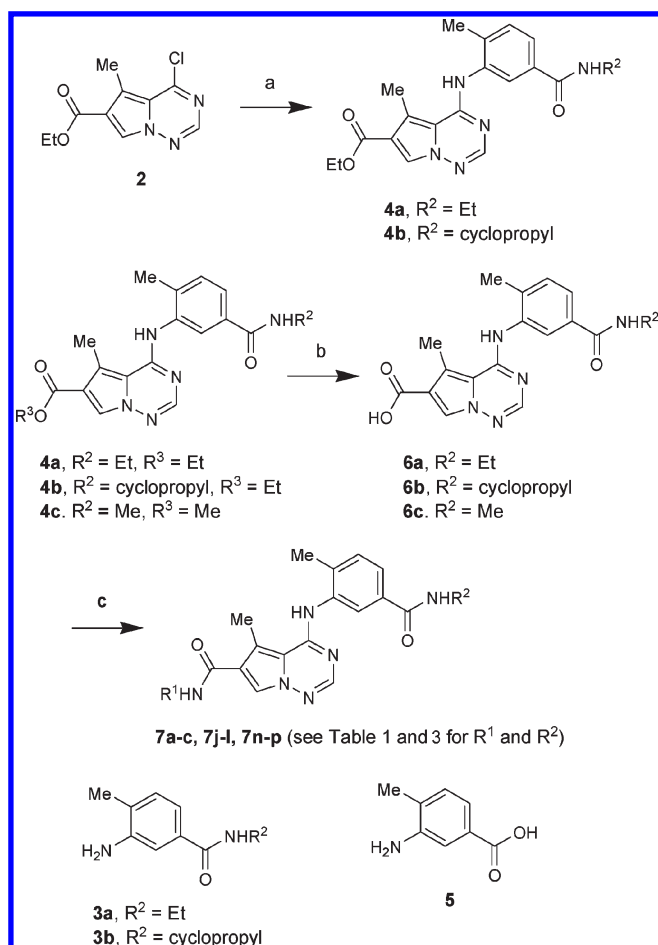
Synthesis of analogues in which the *N*-methoxy group of **1a** and **1b** was replaced was straightforward from previously described advanced intermediates. Analogues **7a–c**, **7j–l**, and **7n–p** were obtained according to Scheme 1. Treatment of ethyl 4-chloro-5-methylpyrrolo[1,2-*f*][1,2,4]triazine-6-carboxylate (**2**)¹² with 3-amino-*N*-ethyl-4-methylbenzamide (**3a**)¹⁴ at room temperature provided **4a**. Similarly, reaction of **2** with 3-amino-*N*-cyclopropyl-4-methylbenzamide (**3b**), which was prepared from 3-amino-4-methylbenzoic acid (**5**) and cyclopropylamine, afforded **4b**. Hydrolysis of **4a–c**¹² supplied acids **6a–c**. Standard coupling reaction conditions using **6a–c** with appropriate amines gave rise to the target amides **7a–c**, **7j–l**, and **7n–p**.

For the preparation of analogues **7d–i**, **7m**, **7q–v** (Scheme 2), we derivatized the previously described compounds **1a–c**.¹² *N*-Methoxybenzamides **1a–c** were treated with methanol in the presence of hydrogen chloride in 1,4-dioxane to yield the corresponding methyl benzoates. The benzoates were then hydrolyzed to give acids **8a–c**. Alternatively, **1a–c** could be directly converted to acids **8a–c** with 1 N hydrochloric acid. Analogues **7d–i**, **7m**, and **7q–v** were obtained from coupling reactions of **8a–c** with the desired amines.

Results and Discussion

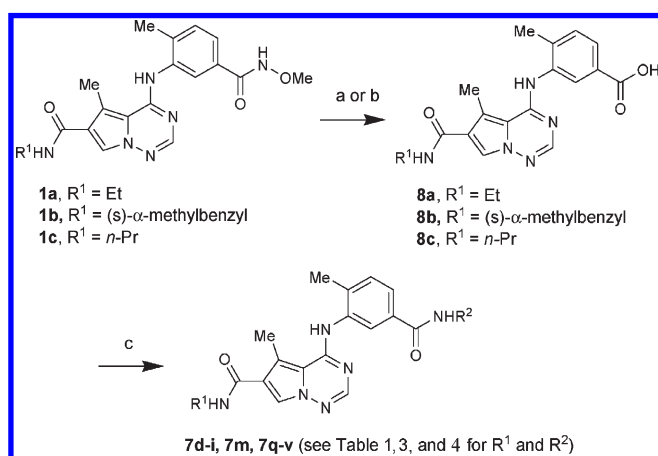
We initially investigated the replacement of the methyl hydroxamate with alkyl amides (Table 1). Replacing the *N*-methoxy group in **1a** with *N*-ethyl resulted in over 35-fold loss in p38α activity, as **7a** inhibited p38α with an IC₅₀ of 110 nM versus 3.1 nM for **1a**. Similarly, the ethyl counterpart of **1b** (**7b**, p38α IC₅₀ = 64.9 nM) was nearly 30-fold less potent than **1b** (p38α IC₅₀ = 2.2 nM). In human peripheral blood mononuclear cells (hPBMC), **7b** inhibited LPS-induced TNFα production with an IC₅₀ of 380 nM, which was 38-fold less

Scheme 1^a



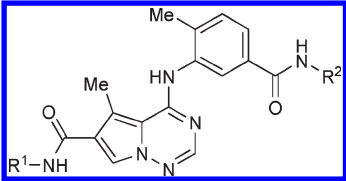
^a Reagent and conditions: (a) *N*-ethyl-3-amino-4-methylbenzamide (**3a**) or *N*-cyclopropyl-3-amino-4-methylbenzamide (**3b**), DMF, rt, overnight, 80% yield; (b) NaOH, THF, 50 °C to reflux, 94–100% yield; (c) R¹NH₂, coupling reagents such as EDC, HOBT, and BOP.

Scheme 2^a



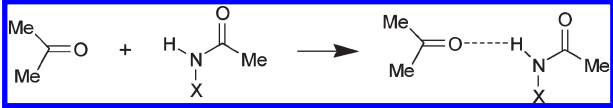
^a Reagent and conditions: (a) (i) MeOH, 4 N HCl in 1,4-dioxane, rt, 16 h, (ii) KOH, 50 °C, 3 h, 71–99% yields; (b) 1 N HCl, reflux, 6.5 h, 95% yield; (c) R²NH₂, coupling reagents such as EDC, HATU, and BOP.

effective than **1b**. Nevertheless, **7a** and **7b** appeared to be the best *N*-alkyl analogues evaluated. The methyl, *n*-propyl, and *i*-propyl amides **7c–e** displayed p38α IC₅₀ values of 397, 166, and 259 nM, respectively, while the *n*-butyl and methoxyethyl

Table 1. in Vitro Activity of **7a–g** vs **1a** and **1b**


compd	R ¹	R ²	p38α IC ₅₀ (nM) ^a	hPBMC TNFα IC ₅₀ (nM) ^b
1a	Et	OMe	3.1	61
1b	(<i>S</i>)-α-methylbenzyl	OMe	2.2	10
7a	Et	Et	110	
7b	(<i>S</i>)-α-methylbenzyl	Et	65	380
7c	Et	Me	397	
7d	<i>n</i> -Pr	<i>n</i> -Pr	166	
7e	Et	<i>i</i> -Pr	259	
7f	Et	<i>n</i> -Bu	>1000	
7g	Et	CH ₂ CH ₂ OMe	>1000	

^a *n* = 4, variation in individual values, <20%. ^b *n* = 3, variation in individual values, <25%.

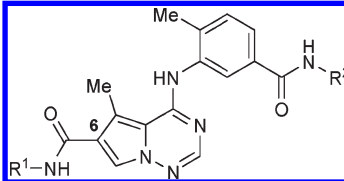
Table 2. Heat of Formation of Hydrogen Bonding


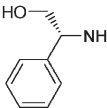
X	MeO	Et	<i>c</i> -Pr
heat of formation (kcal/mol) ^a	−6.72 ^b	−4.86	−5.06

^a Acetone and *N*-substituted acetamide were first minimized using SAM1, and then the minimized complex were subjected to geometry optimization in vacuo using DFT B3LYP/6-31+g(d,p) as implemented within Jaguar. Hydrogen bond heats of formation were calculated as the difference between components (acetone and *N*-substituted acetamide and the complex). ^b Model complex includes an additional interaction between the acetone methyl hydrogens and methoxy oxygen.

analogues **7f** and **7g** both inhibited p38α with IC₅₀ values of greater than 1000 nM.

In considering the suboptimal potency of the *N*-ethylbenzamide **7a** relative to the *N*-methoxybenzamide **1a**, we speculated that the *N*-methoxy oxygen of **1a** could make the amide NH an excellent hydrogen bond donor due to its electron withdrawing nature. Previously, X-ray crystallographic analysis of **1a** bound to p38α had revealed that the *N*-methoxybenzamide NH in **1a** forms a key hydrogen bond with Glu 71 of p38α.¹² Computations using *N*-substituted acetamide as a hydrogen bond donor and acetone as a hydrogen bond acceptor indicated that the heat of formation of hydrogen bonding between *N*-methoxyacetamide NH and acetone carbonyl oxygen was −6.72 kcal/mol. The corresponding hydrogen bond between *N*-ethyl acetamide and acetone had a heat of formation of −4.86 kcal/mol (Table 2). Assuming that the interaction between the acetone methyl hydrogens and methoxy oxygen is negligible relative to the H-bonding component, these results suggested that the *N*-methoxybenzamide NH in **1a** could form a much stronger hydrogen bond with Glu 71 of p38α than the *N*-ethylbenzamide NH in **7a**. As a result of this analysis, replacement of *N*-methoxy in **1a** with *N*-cyclopropyl was specifically proposed, rationalizing that the sp² character of the cyclopropyl carbons would make the benzamide NH a stronger hydrogen bond donor. Similar computational analysis determined that the heat of formation of hydrogen bonding

Table 3. in Vitro Activity of **7h–p**


compd	R ¹	R ²	P38α IC ₅₀ (nM) ^a	hPBMC TNFα IC ₅₀ (nM) ^b
7h	Et	<i>c</i> -Pr	18	191
7i	Et	<i>c</i> -Bu	222	
7j	Me	<i>c</i> -Pr	24	225
7k	<i>n</i> -Pr	<i>c</i> -Pr	13	50
7l	<i>n</i> -Bu	<i>c</i> -Pr	10	81
7m	(<i>S</i>)-α-methylbenzyl	<i>c</i> -Pr	12	64
7n	(<i>S</i>)- <i>sec</i> -Bu	<i>c</i> -Pr	27	58
7o	MeOCH ₂ CH ₂	<i>c</i> -Pr	31	188
7p		<i>c</i> -Pr	41	543

^a *n* = 4, variation in individual values, <20%. ^b *n* = 3, variation in individual values, <25%.

between *N*-cyclopropylacetamide NH and acetone carbonyl oxygen was −5.06 kcal/mol (Table 2). This implied that the activity of the *N*-cyclopropylbenzamide analogues might lie between that observed for the *N*-methoxybenzamide and the *N*-ethylbenzamide analogues. It was hoped that the *N*-cyclopropylbenzamide analogues might also show improved pharmacokinetic properties, resulting in similar or better efficacy relative to **1a**.

We were encouraged that the *N*-cyclopropylbenzamide **7h** displayed a p38α IC₅₀ value of 18 nM (Table 3). Thus, as predicted, it was ~6-fold less potent than the *N*-methoxybenzamide and ~5.5-fold more potent than the *N*-ethylbenzamide. Compound **7h** also inhibited LPS-induced TNFα production in hPBMC with an IC₅₀ of 191 nM. In contrast, the closely related *N*-cyclobutylbenzamide analogue **7i** was determined to be 12-fold less active against p38α relative to **7h**, with an IC₅₀ value of 222 nM.

With *N*-cyclopropyl being identified as a suitable replacement for *N*-methoxy in **1a**, our attention was then focused on optimization of the 6-carboxamide substitution in the *N*-cyclopropyl amide series (Table 3). The use of 6-*N*-methyl amide in place of *N*-ethyl resulted in a slight drop in both enzymatic and cellular activities, as **7j** inhibited p38α with an IC₅₀ of 24 nM and TNFα production in hPBMC with an IC₅₀ of 225 nM. However, when the 6-*N*-ethyl group in **7h** was replaced with certain more hydrophobic alkyl groups, the resulting analogues displayed improved activities in both the enzymatic and cellular assays. For example, the *N*-propyl 6-carboxamide analogue **7k** displayed a p38α IC₅₀ of 13 nM and a cellular TNFα IC₅₀ of 50 nM. Similarly, the enzymatic and cellular IC₅₀ values for the *N*-butyl 6-carboxamide analogue **7l** were determined to be 9.7 and 81 nM, respectively. Also, the *N*-(*S*)-α-methylbenzyl 6-carboxamide analogue **7m** (p38α IC₅₀ = 12 nM, TNFα IC₅₀ = 64 nM), the *N*-cyclopropylbenzamide counterpart of **1b**, was a potent p38α inhibitor and very effective in cells. The *N*-(*S*)-*sec*-butyl 6-carboxamide analogue **7n** appeared to be less potent against p38α (IC₅₀ = 27 nM) than **7m**, but its cellular potency (TNFα IC₅₀ = 57 nM) was very comparable to what was observed with **7m**. In contrast, introducing polar functionality in the

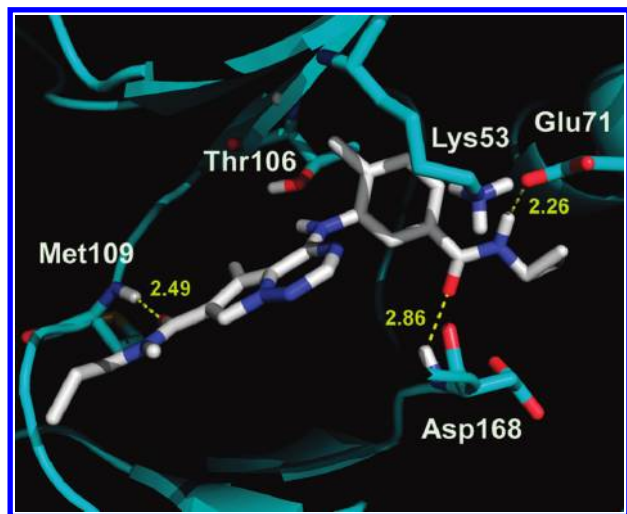


Figure 3. X-ray crystallographic structure of **7k** bound to p38 α .

6-carboxamide moiety generally led to decreased activities in the enzymatic and cellular assays, as demonstrated by **7o** (p38 α IC₅₀ = 31 nM, TNF α IC₅₀ = 188 nM) and **7p** (p38 α IC₅₀ = 41 nM, TNF α IC₅₀ = 543 nM). Notably, even though **7k–m** are 3–9-fold less potent against p38 α compared to **1a**, their cellular activities are comparable to that of **1a**. This result may be related to the improved permeability of analogues **7k–m** compared to **1a**. Consistent with that assumption, the Caco-2 transcellular permeability was found to be in a range of 91–134 nm/s for **7k** versus only 5 nm/s for **1a**.

As anticipated, and shown by the X-ray cocrystal structure of **7k** with p38 α enzyme (Figure 3), the binding mode of the *N*-cyclopropylbenzamide is similar to that observed with **1a**. The benzamide moiety provides two key hydrogen bond interactions with p38 α : the carbonyl oxygen interaction with Asp168 (2.86 Å) and the NH interaction with Glu 71 (2.26 Å). Another important hydrogen bond interaction occurs between the 6-carboxamide oxygen and the Met 109 (2.49 Å) at the hinge region. Hydrophobic interactions include the angular methylaniline moiety being positioned within a hydrophobic pocket and the pendant *N*-propyl interacting with a hydrophobic site characteristically found at the outer rim of the hinge region.

We also examined the replacement of the methyl hydroxamate with aryl amides (Table 4). The *N*-phenyl amide **7q** exhibited a p38 α IC₅₀ value of 50 nM, which was less potent than *N*-methoxybenzamide **1b** or *N*-cyclopropylbenzamide **7m** and essentially equipotent with *N*-ethylbenzamide **7b**. Our modeling studies suggested that the *N*-phenyl group was a little too large to fit into the binding pocket. This also explained the p38 α activity (IC₅₀ = 72 nM) for *N*-2-thiazolylbenzamide **7r** because the actual dimensions of phenyl and thiazolyl are very similar. The cellular TNF α IC₅₀ values of **7q** and **7r** were both determined to be greater than 1000 nM. When a methyl was added to the thiazole ring in **7r**, the resulting analogue **7s** displayed a p38 α IC₅₀ value of over 1000 nM. Analogue **7t** containing a smaller *N*-oxazolyl group in the benzamide moiety provided an improved p38 α IC₅₀ value of 35 nM. However, the *N*-3-isoxazolylbenzamides were found to be highly potent against p38 α , as **7u** and **7v** inhibited p38 α with IC₅₀ values of 7.1 and 3.9 nM, respectively. These two inhibitors were also extremely active at inhibiting TNF α production in hPBMC, exhibiting IC₅₀ values of 9.7 and 6.0 nM, respectively. The significant improvement in binding affinity for **7u** and **7v** compared to **7t** was surprising.

Table 4. In Vitro Activity of **7q–v**

compd	R ¹	R ²	P38 α IC ₅₀ (nM) ^a	hPBMC TNF α IC ₅₀ (nM) ^b
7q	(<i>S</i>)- α -methylbenzyl	Ph	50	1011
7r	Et		72	> 1000
7s	Et		> 1000	
7t	Et		35	604
7u	Et		7.1	9.7
7v	<i>n</i> -Pr		3.9	6.0

^a *n* = 4, variation in individual values, < 20%. ^b *n* = 3, variation in individual values, < 25%.

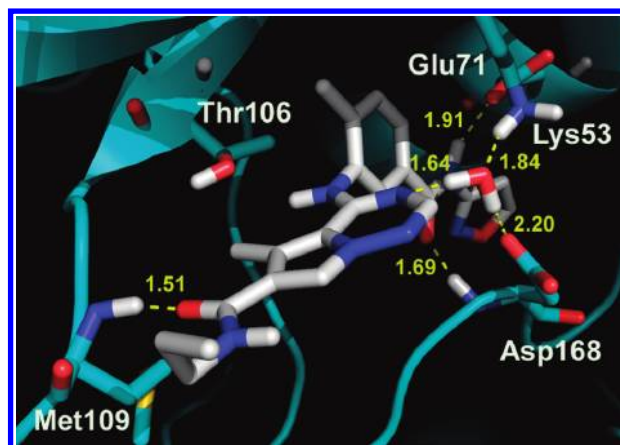


Figure 4. X-ray crystallographic structure of **7v** bound to p38 α .

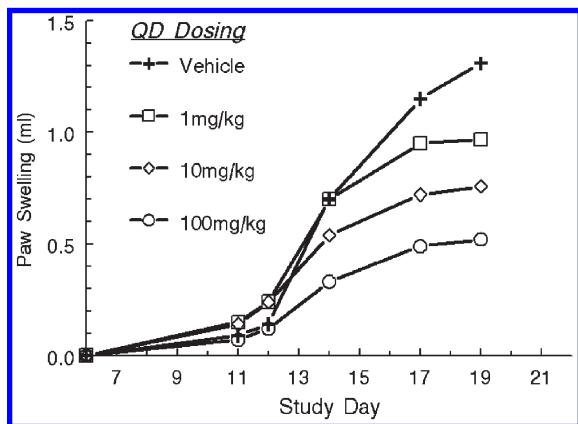
A cocrystal of **7v** with p38 α was obtained,¹⁵ and the X-ray crystallographic analysis showed that **7v** bound to p38 α in a similar manner as inhibitor **7k** (Figure 3) except that an active water molecule was engaged with **7v**, Asp168, and Lys 53 (Figure 4).

On the basis of cellular activity and other profiling data (e.g., liver microsomal stability and P450 inhibition), selected compounds were evaluated in a murine model of acute inflammation. In this study, compounds were administered to mice prior to challenging with LPS. Ninety minutes postdose, plasma samples were taken and analyzed for TNF α levels. In addition to a vehicle group, **1a** was included as a comparator and positive control in each study. Compounds were considered active if they reduced the LPS induced TNF α production by 50%. As seen in Table 5, when dosed at 5 mg/kg, 2 h prior to LPS challenge, compounds **7k**, **7l**, **7u**, and **7v** all showed improved efficacy relative to **1a**, inhibiting the TNF α levels by 77–92% (versus 65–66% inhibition with **1a**). The weakest compound studied in this protocol was **7o** (41% reduction of TNF α). To differentiate these active compounds, they were further examined under a more stringent protocol, wherein the

Table 5. Inhibition of LPS Induced TNF α Production in Mice^a

compd	dose (mg/kg) ^a	dosing interval prior to LPS (hr)	percent inhibition ^b	percent inhibition for 1a
7k	5	2	89	66
7l	5	2	77	66
7o	5	2	41	65
7u	5	2	92	65
7v	5	2	78	66
7k	5	6	78	50
7l	5	6	27	50
7u	5	6	89	63
7v	5	6	83	50

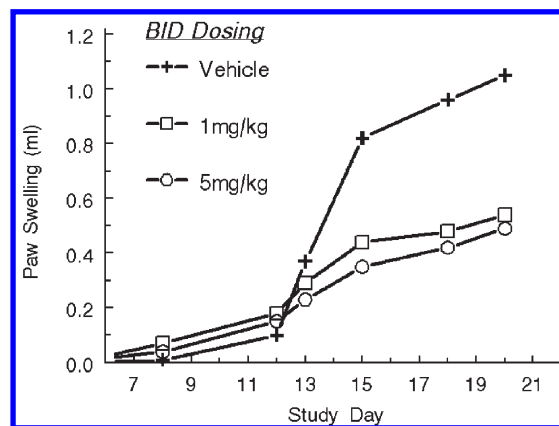
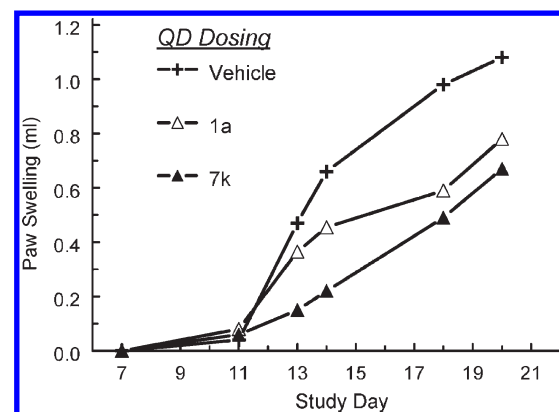
^a PEG 300 was used as the vehicle, 6–8 mice per group. ^b Percent inhibition was calculated relative to vehicle group.

**Figure 5.** Compound **7k** in the rat adjuvant arthritis model (qd dosing). Vehicle: PEG 300.

dosing interval was extended to 6 h prior to LPS challenge. Under this protocol, **7k**, **7u**, and **7v** were active, reducing TNF α production by 78%, 89%, and 83%, respectively, with **1a** giving 50–63% reduction of TNF α .

On the basis of the above characterization, inhibitors **7k** and **7u** were chosen to be evaluated in a pseudoestablished rat adjuvant arthritis (rat AA) model. In this study, complete Freund's adjuvant was given to rats at day one and the rats' immune responses were allowed to develop for 10 days. At day 11, the rats started to receive compounds orally and the paw swelling was measured periodically. Though **7u** was very active in the acute murine model of inflammation even when dosed at 5 mpk 6 h prior to LPS challenge, it was not active in the rat AA model when dosed once daily at 10 mg/kg. It was found in this study that **7u** initially provided high drug concentration, but the drug concentration dropped dramatically (by 80%) after 6 h. However, inhibitor **7k** displayed dose-dependent reduction in paw swelling with qd dosing, with efficacy observed at doses of 10 and 100 mg/kg (Figure 5). With bid dosing, **7k** showed improved efficacy, achieving marked reduction in paw swelling at doses of 1 and 5 mg/kg (Figure 6). Statistically significant reduction in paw swelling was also observed at doses as low as 0.3 mg/kg bid. In addition, it was demonstrated that **7k** was more effective than **1a** in the rat AA model at a dose of 10 mg/kg qd (Figure 7).

Inhibitor **7k** is approximately 4-fold less potent against p38 α than **1a**, but **7k** is more effective than **1a** in both the acute and chronic disease models. This is likely due to the significantly improved pharmacokinetic profile of **7k** (Table 6) relative to **1a**. The most significant improvement was the dramatically reduced clearance rate which resulted in significantly increased exposure. For example, the mouse clearance rate for **7k** was

**Figure 6.** Compound **7k** in the rat adjuvant arthritis model (bid dosing). Vehicle: PEG 300.**Figure 7.** Compound **7k** vs **1a** in the rat adjuvant arthritis model (qd dosing). Vehicle: PEG 300.**Table 6.** Pharmacokinetic Properties of **7k** in Mice^a and Rats^b

	mouse	rat
% F_{po}	90	60
C_{max} (μ M)	15.3	7.0
T_{max} (h)	1.0	1.5
$T_{1/2}$ (h)	2.6	4.0
MRT (h)	3.3	3.4
CL (mL/min/kg)	4.4	5.4
V_{ss} (L/kg)	0.9	1.1
$AUC_{0-8 h}$ (μ M \cdot h)	75.5	
$AUC_{0-24 h}$ (μ M \cdot h)		45.4

^a Vehicle: 20% NMP, 35% PEG 400, 10% PG, and 35% water for iv, and PEG 400 for po; dose: 5 mg/kg for iv, and 10 mg/kg for po; 3 mice per group. ^b Vehicle: 25% NMP, 33% PEG 400, 9% PG, and 33% water for iv, and PEG 400 for po; dose: 2.5 mg/kg for iv, and 10 mg/kg for po; 3 mice per group.

4.4 mL/min/kg versus 93 mL/min/kg for **1a**. And, at an oral dose of 10 mg/kg, the mouse $AUC_{0-8 h}$ for **7k** was 75.5 μ M \cdot h versus 3.6 μ M \cdot h. Compound **7k** exhibited oral bioavailability values of 90% and 60% in mice and rats, respectively.

Table 7 contains the in vitro profile of **7k**. The compound had a low rate of oxidative metabolism in mouse (0.011 nmol/min/mg), rat (0.008 nmol/min/mg), and human liver microsomes (0.013 nmol/min/mg). The metabolic rate in hepatocytes was also low in these species. Compound **7k** did not significantly inhibit cytochrome P450 isozymes 1A2, 2C9, 2C19, and 2D6 with IC_{50} values $> 40 \mu$ M. It was a weak inhibitor of CYP3A4, with an IC_{50} value ranging from 18 to 40 μ M based in multiple tests. As mentioned earlier, the Caco-2 permeability of **7k** was

Table 7. In Vitro Profile of **7k**

profiling assays	results
liver microsome metabolic rate (nmol/min/mg)	mouse: 0.011 rat: 0.008 human: 0.013
hepatocyte metabolic rate (nmol/min/million cells)	mouse: 0.006 rat: 0.015 human: 0.015
P450 IC ₅₀ (μM)	>40 for 1A2, 2C9, 2C19, and 2D6 18–40 for 3A4
Caco-2 permeability (nm/s)	121–134
serum protein binding (%)	mouse: 86.3 rat: 89.7 human: 81.5
Ames	negative in T98 and T100 ± S9 activation
SOS chromotest	negative
HHA IC ₅₀ (μM)	>138
hERG inhibition	16% at 30 μM
kinase selectivity	>2000 fold over 57 diverse kinases 450 fold over Jnk2 190 fold over Raf 5 fold over p38β

determined to be in a range of 91–134 nm/s. The serum protein binding for **7k** at 10 μM was 86%, 90%, and 82% in fresh sera isolated from mice, rats, and humans, respectively. The compound was negative in the Ames reverse-mutation and SOS chromotest assays. Also, **7k** was not cytotoxic in the human hepatotoxicity assay (HHA) (IC₅₀ > 138 μM for all isoforms), suggesting a decreased likelihood for clinical hepatic liabilities. In addition, **7k** only minimally inhibited hERG current in a patch clamp assay (16% at 30 μM). The compound proved to be highly selective over other kinases tested. It displayed >2000-fold selectivity for p38α over a diverse panel of 57 kinases that include serine kinases, nonreceptor tyrosine kinases, receptor tyrosine kinases, and the p38γ and δ isoforms. Compound **7k** was also 450-fold selective over Jnk2, a MAP kinase involved in inflammation, and 190-fold selective over Raf. However, **7k** showed only 5-fold selectivity over p38β. On the basis of its safety profile in preclinical safety studies, compound **7k**, also designated as BMS-582949, was nominated for further development and clinical studies in inflammatory disease.

In summary, to improve the pharmacokinetic properties of our previously reported p38α MAP kinase inhibitors, the *N*-methoxy moiety in **1a** and **1b** was replaced with an *N*-cyclopropyl group. This specific modification was based on our hypothesis that the π-character of the cyclopropyl moiety would enhance the hydrogen bonding ability of the benzamide NH in comparison to the less potent *N*-alkyl analogues. This proposal ultimately led to the discovery of **7k**, a highly selective p38α inhibitor. Compared to **1a**, **7k** displayed a significantly improved pharmacokinetic profile and was more effective in both the acute murine model of inflammation and rat adjuvant arthritis model despite its slightly reduced potency. Compound

7k is currently in phase II clinical trials for the treatment of rheumatoid arthritis, the results of which will be reported in due course.

Experimental Section

Chemistry. Proton and carbon magnetic resonance (¹H and ¹³C NMR) spectra were recorded either on a Bruker Avance 400 or a JEOL Eclipse 500 spectrometer and are reported in ppm relative to the reference solvent of the sample in which they were run. HPLC and LCMS analyses were conducted using a Shimadzu LC-10AS liquid chromatograph and a SPD UV–vis detector at 220 or 254 nm with the MS detection performed with a Micromass Platform LC spectrometer. HPLC analyses were performed using the following conditions: Ballistic YMC S5 ODS 4.6 mm × 50 mm column with a binary solvent system where solvent A = 10% methanol, 90% water, 0.2% phosphoric acid, and solvent B = 90% methanol, 10% water, and 0.2% phosphoric acid, flow rate = 4 mL/min, linear gradient time = 4 min, start %B = 0, final %B = 100. All final compounds had an HPLC purity of ≥95% unless specifically mentioned. LCMS analyses were performed using the following conditions: Phenomenex 5 μm C18 4.6 mm × 50 mm column with a binary solvent system where solvent A = 10% methanol, 90% water, 0.1% trifluoroacetic acid, and solvent B = 90% methanol, 10% water, and 0.1% trifluoroacetic acid, flow rate = 4 mL/min, linear gradient time = 2 min, start %B = 0, final %B = 100. Preparative reverse-phase HPLC purifications were performed using the following conditions: Ballistic YMC S5 ODS 20 mm × 100 mm column with a binary solvent system where solvent A = 10% methanol, 90% water, 0.1% trifluoroacetic acid, and solvent B = 90% methanol, 10% water, and 0.1% trifluoroacetic acid, flow rate = 20 mL/min, linear gradient time = 10 min, start %B = 20, final %B = 100.

All reagents were purchased from commercial sources and used without further purification unless otherwise noted. All reactions were performed under an inert atmosphere. Reactions run in aqueous media were run under an ambient atmosphere unless otherwise noted.

3-Amino-*N*-cyclopropyl-4-methylbenzamide (3b). To a solution of 3-amino-4-methylbenzoic acid (**5**) (5.12 g, 33.9 mmol), 1-(3-dimethylaminopropyl)-3-ethylcarbodiimide hydrochloride (EDC) (9.97 g, 52.0 mmol), and 4-(dimethylamino)pyridine (0.89 g, 7.3 mmol) in DMF (100 mL) at 0 °C was added cyclopropylamine (4.0 mL, 57.7 mmol) dropwise. After stirring for 15 min, the cold bath was removed and the reaction mixture was stirred at room temperature overnight. Volatiles were removed under vacuum, and the residue was diluted with water and extracted with dichloromethane (3 times). The organic layers were combined, dried over sodium sulfate, and concentrated under vacuum. The residue was subjected to silica gel chromatography using dichloromethane/methanol (20:1) as eluent to afford the title compound (6.98 g, 108% yield) as a yellow oil. This product was contaminated with dimethylformamide but used in the next step without further purification. LCMS (EI) *m/z* Calcd for C₁₁H₁₄N₂O (M + H)⁺ = 191.11. Found: 192.09.

Ethyl 4-(5-(Ethylcarbamoyl)-2-methylphenylamino)-5-methylpyrrolo[1,2-*f*][1,2,4]triazine-6-carboxylate (4a). To a mixture of ethyl 4-chloro-5-methylpyrrolo[1,2-*f*][1,2,4]triazine-6-carboxylate (**2**) (4.83 g, 20.2 mmol) and the HCl salt of 3-amino-*N*-ethyl-4-methylbenzamide (**3a**)¹² (4.33 g, 20.2 mmol) in DMF (70 mL) was added diisopropylethylamine (2.80 mL, 16.2 mmol). The resulting mixture was heated at 60 °C for 5 h, then cooled to rt and slowly added to a mixture of crushed ice (100 mL) and saturated aqueous NaHCO₃ solution (200 mL). After stirring overnight, the solid was collected by suction filtration and rinsed with water (200 mL) to afford a pale-yellow solid. Recrystallization from ethanol/water (1:1) afforded the title compound (5.50 g, 71%) as white crystals. LCMS (EI) *m/z* Calcd for C₂₀H₂₃N₅O₃ (M + H)⁺ = 382.28. Found: 382.30.

Ethyl 4-(5-(Cyclopropylcarbamoyl)-2-methylphenylamino)-5-methylpyrrolo[1,2-*f*][1,2,4]triazine-6-carboxylate (4b). A solution

of ethyl 4-chloro-5-methylpyrrolo[1,2-*f*][1,2,4]triazine-6-carboxylate (**2**) (1.30 g, 5.40 mmol) and 3-amino-*N*-cyclopropyl-4-methylbenzamide (**3b**) (1.60 g, 8.40 mmol) in DMF (13 mL) was stirred at room temperature overnight. Water was added, and the precipitated product (1.70 g, 80% yield) was collected as an off-white solid by filtration, followed by trituration with diethyl ether. LCMS (EI) *m/z* Calcd for C₂₁H₂₃N₅O₃ (M + H)⁺ = 394.18. Found: 394.31.

4-(5-(Ethylcarbamoyl)-2-methylphenylamino)-5-methylpyrrolo[1,2-*f*][1,2,4]triazine-6-carboxylic Acid (6a). To a solution of ethyl 4-(5-(ethylcarbamoyl)-2-methylphenylamino)-5-methylpyrrolo[1,2-*f*][1,2,4]triazine-6-carboxylate (**4a**) (1.81 g, 4.74 mmol) in THF/MeOH (1:1 v/v, 7 mL) at rt was added aqueous 3 N KOH solution (4.7 mL, 14.2 mmol). The reaction mixture was stirred at 60 °C for 6 h, then concentrated under vacuum to remove THF and methanol. The residue was cooled at 0 °C, and the pH value was adjusted to ~3 by addition of aqueous 6 N HCl. The resulting solid was collected by filtration, washed with water (5 mL × 3), and dried under vacuum to afford the title compound (1.64 g, 90% yield) as a white solid. LCMS (EI) *m/z* Calcd for C₁₈H₁₉N₅O₃ (M + H)⁺ = 354.15. Found: 354.30.

4-(5-(Cyclopropylcarbamoyl)-2-methylphenylamino)-5-methylpyrrolo[1,2-*f*][1,2,4]triazine-6-carboxylic Acid (6b). A mixture of ethyl 4-(5-(cyclopropylcarbamoyl)-2-methylphenylamino)-5-methylpyrrolo[1,2-*f*][1,2,4]triazine-6-carboxylate (**4b**) (5.00 g, 12.7 mmol) and 1 N NaOH solution (51 mL, 51 mmol) in THF (30 mL) was heated at reflux for 16 h, then concentrated under vacuum. The residue was extracted with ethyl acetate. The aqueous solution was neutralized with aqueous 6 N HCl solution to pH 6. The precipitating product (4.35 g, 94% yield) was collected as a white solid by suction filtration, washed with water, and dried over Drierite under vacuum. ¹H NMR (400 MHz, DMSO-*d*₆/D₂O) δ 8.46 (s, 1H), 8.02 (s, 1H), 7.84 (s, 1H), 7.78 (s, 1H), 7.67 (d, *J* = 7.8 Hz, 1H), 7.38 (d, *J* = 7.8 Hz, 1H), 2.83 (m, 1H), 2.81 (s, 3H), 2.22 (s, 3H), 0.69 (m, 2H), 0.55 (m, 2H).

5-Methyl-4-(2-methyl-5-(methylcarbamoyl)phenylamino)pyrrolo[1,2-*f*][1,2,4]triazine-6-carboxylic Acid (6c). To a solution of methyl 5-methyl-4-(2-methyl-5-(methylcarbamoyl)phenylamino)pyrrolo[1,2-*f*][1,2,4]triazine-6-carboxylate (**4c**) (0.17 g, 0.48 mmol) in THF (1 mL) was added aqueous 1 N NaOH solution (1.0 mL, 1.0 mmol). The homogeneous solution was stirred at 50 °C. Upon complete conversion by HPLC analysis, aqueous 1 N HCl was slowly added with vigorous stirring to give a precipitate. The mixture was agitated for 2 h, then the precipitate was collected by filtration to afford the title compound as a tan solid in quantitative yield (92% purity by HPLC analysis). The material was used directly for the next step without further purification.

3-(6-(Ethylcarbamoyl)-5-methylpyrrolo[1,2-*f*][1,2,4]triazin-4-ylamino)-4-methylbenzoic Acid (8a). To a slurry of *N*-ethyl-4-(5-(methoxycarbamoyl)-2-methylphenylamino)-5-methylpyrrolo[1,2-*f*][1,2,4]triazine-6-carboxamide (**1a**)¹² (2.0 g, 4.20 mmol) in anhydrous methanol (12 mL) was added a solution of HCl in dioxane (4 N, 18 mL, 72 mmol) at rt. The resulting clear solution was stirred at rt for 16 h, then concentrated under vacuum. The resulting oil was dissolved in aqueous 1.5 N potassium hydroxide solution (16 mL) and heated to 50 °C for 3 h. After cooling to rt, the mixture was diluted with water (50 mL) and 10% aqueous HCl was added until pH was approximately 3 or 4. The precipitating product was collected by vacuum filtration, washed with water (50 mL), and dried under vacuum to afford the title product (1.47 g, 99% yield) as a white solid. An analytical sample was obtained after recrystallization from 10% aqueous acetonitrile. LCMS (EI) *m/z* Calcd for C₁₈H₁₉N₅O₃ (M + H)⁺ = 354.15. Found: 354.20. ¹H NMR (400 MHz, CD₃OD) δ 8.21 (br s, 1H), 8.11 (br s, 1H), 7.89–7.91 (m, 2H), 7.67 (br s, 1H), 7.44 (d, 1H), 3.40 (q, 2H), 2.86 (s, 3H), 2.36 (s, 3H), 1.25 (s, 3H).

(S)-4-Methyl-3-(5-methyl-6-(1-phenylethylcarbamoyl)pyrrolo[1,2-*f*][1,2,4]triazin-4-ylamino)benzoic Acid (8b). This compound was prepared from (*S*)-4-(5-(methoxycarbamoyl)-2-methylphenylamino)-5-methyl-*N*-(1-phenylethyl)pyrrolo[1,2-*f*][1,2,4]triazine-6-carboxamide (**1b**) in the same way as **8a** was from **1a**;

yield 71%. ¹H NMR (MeOD) δ 8.54 (br s, 1H), 8.12 (br s, 1H), 8.02 (br s, 1H), 7.88 (br s, 1H), 7.69 (br s, 1H), 7.41–7.44 (m, 3H), 7.32–7.36 (m, 2H), 7.22–7.26 (m, 1H), 5.19–5.27 (m, 1H), 2.81 (s, 3H), 2.34 (s, 3H), 1.56 (d, *J* = 7.1 Hz, 3H).

4-Methyl-3-(5-methyl-6-(propylcarbamoyl)pyrrolo[1,2-*f*][1,2,4]triazin-4-ylamino)benzoic Acid (8c). A solution of *N*-*n*-propyl-4-(2-methyl-5-(methoxycarbamoyl)phenylamino)-5-methylpyrrolo[1,2-*f*][1,2,4]triazine-6-carboxamide (**1c**) (2.28 g) in aqueous 1 N HCl (30 mL) was heated at 85 °C for 6.5 h. Upon cooling to rt, the mixture was neutralized with aqueous 1 N NaOH solution to pH 6. The precipitating product (1.60 g, 95% yield) was collected by suction filtration and dried. LCMS (EI) *m/z* Calcd for C₁₉H₂₁N₅O₃ (M + H)⁺ = 368.10. Found: 368.17. NMR (400 MHz, MeOD) δ 8.20 (br s, 1H), 8.12 (br s, 1H), 7.92–7.89 (m, 2H), 7.69 (br s, 1H), 7.45 (d, *J* = 8.0 Hz, 1H), 3.35 (m, 2H), 2.86 (s, 3H), 2.36 (s, 3H), 1.67 (m, 2H), 1.02 (t, *J* = 7.5 Hz, 3H).

***N*-Ethyl-4-(5-(ethylcarbamoyl)-2-methylphenylamino)-5-methylpyrrolo[1,2-*f*][1,2,4]triazine-6-carboxamide (7a).** To a solution of 4-(5-(ethylcarbamoyl)-2-methylphenylamino)-5-methylpyrrolo[1,2-*f*][1,2,4]triazine-6-carboxylic acid (**6a**) (20.0 mg, 0.057 mmol) in DMF (0.30 mL) were added HOBt (9.1 mg, 0.068 mmol) and EDC (13.0 mg, 0.068 mmol). The resulting solution was stirred at rt for 1 h before ethylamine hydrochloride (12.6 mg, 0.068 mmol) and diisopropylethylamine (24 μL, 0.14 mmol) were added. The mixture was stirred at rt for 16 h, then subjected to preparative HPLC to afford a TFA salt of the title compound (10.0 mg, 46% yield) as a white solid; 97% purity by HPLC. LCMS (EI) *m/z* Calcd for C₂₀H₂₄N₆O₂ (M + H)⁺ = 381.20. Found: 381.10. ¹H NMR (400 MHz, MeOD) δ 7.85 (s, 1H), 7.76 (s, 1H), 7.62 (d, *J* = 8.0 Hz, 1H), 7.65 (s, 1H), 7.33 (d, *J* = 8.0 Hz, 1H), 3.32–3.26 (m, 4H), 2.74 (s, 3H), 2.23 (s, 3H), 1.13 (t, *J* = 7.2 Hz, 3H), 1.11 (t, *J* = 7.2 Hz, 3H).

(S)-4-(5-(Ethylcarbamoyl)-2-methylphenylamino)-5-methyl-*N*-(1-phenylethyl)pyrrolo[1,2-*f*][1,2,4]triazine-6-carboxamide (7b). To a solution of 4-(5-(ethylcarbamoyl)-2-methylphenylamino)-5-methylpyrrolo[1,2-*f*][1,2,4]triazine-6-carboxylic acid (**6a**) (20 mg, 0.056 mmol) in DMF (0.3 mL) were successively added HOBt (8.4 mg, 0.062 mmol) and EDC (12 mg, 0.062 mmol). The resulting solution was stirred at rt for 1 h before (*S*)-α-methylbenzylamine (14 μL, 0.112 mmol) was added. After stirring at rt for 16 h, the mixture was subjected to preparative HPLC to obtain a TFA salt of the title compound (13.0 mg, 52% yield) as a white solid; 99% purity by HPLC. LCMS (EI) *m/z* Calcd for C₂₆H₂₈N₆O₂ (M + H)⁺ = 457.23. Found: 457.30. ¹H NMR (400 MHz, MeOD) δ 8.12 (s, 1H), 7.90 (s, 1H), 7.78 (d, *J* = 8.0 Hz, 1H), 7.71 (s, 1H), 7.49 (d, *J* = 8.0 Hz, 1H), 7.44–7.43 (m, 2H), 7.38–7.35 (m, 2H), 7.26 (m, 1H), 5.25 (q, *J* = 7.0 Hz, 1H), 3.43 (q, *J* = 7.3 Hz, 2H), 2.84 (s, 3H), 2.36 (s, 3H), 1.58 (d, *J* = 7.0 Hz, 3H), 1.24 (t, *J* = 7.3 Hz, 3H).

***N*-Ethyl-5-methyl-4-(2-methyl-5-(methylcarbamoyl)phenylamino)-pyrrolo[1,2-*f*][1,2,4]triazine-6-carboxamide (7c).** To a solution of 5-methyl-4-(2-methyl-5-(methylcarbamoyl)phenylamino)pyrrolo[1,2-*f*][1,2,4]triazine-6-carboxylic acid (**6c**) (0.15 g, 0.442 mmol) in DMF (2.5 mL) was added BOP (0.215 g, 0.486 mmol). In a second vial, ethylamine hydrochloride (0.072 g, 0.884 mmol) was dissolved in DMF (0.5 mL) and DIPEA (0.15 mL, 0.884 mmol), and 0.50 mL of the acid (**6c**)/BOP solution was introduced. The reaction was agitated at room temperature overnight and then diluted slowly with water (5 mL) with vigorous stirring and cooling in an ice bath. The resulting solid was collected by filtration and air-dried to afford the title compound (0.0267 g, 82% yield) as an off-white solid. LCMS (EI) *m/z* Calcd for C₁₉H₂₂N₆O₂ (M + H)⁺ = 367.18. Found: 367.10. NMR (400 MHz, MeOD) δ 8.09 (s, 1H), 7.89 (d, *J* = 1.8 Hz, 1H), 7.81 (d, *J* = 8.0 Hz, 1H), 7.73 (s, 1H), 7.54 (d, *J* = 8.0 Hz, 1H), 3.40 (q, *J* = 7.3 Hz, 2H), 2.93 (s, 3H), 2.87 (s, 3H), 2.37 (s, 3H), 1.24 (t, *J* = 7.3 Hz, 3H).

5-Methyl-4-(2-methyl-5-(propylcarbamoyl)phenylamino)-*N*-propylpyrrolo[1,2-*f*][1,2,4]triazine-6-carboxamide (7d). To a solution of 4-methyl-3-(5-methyl-6-(propylcarbamoyl)pyrrolo[1,2-*f*][1,2,4]triazin-4-ylamino)benzoic acid (**8c**) (47.5 mg, 0.13 mmol)

in DMF (0.4 mL) were added HOBt (21 mg, 0.16 mmol) and EDC (30 mg, 0.16 mmol), and the solution was stirred for 2 h. *n*-Propylamine (21.4 μ L, 0.26 mmol) was added, and the mixture was stirred for 15 h. Water (0.4 mL) was added and the precipitated solids were collected by filtration, washed with water, and dried under vacuum to afford the title compound (45 mg, 85% yield) as a white solid; 96% purity by HPLC. LCMS (EI) m/z Calcd for $C_{22}H_{28}N_6O_2$ ($M + H$)⁺ = 409.10. Found: 409.20. ¹H NMR (400 MHz, DMSO-*d*₆) δ 8.49 (s, 1H), 8.25 (br m, 1H), 7.93 (m, 2H), 7.75 (s, 1H), 7.61 (s, 1H), 7.53 (d, J = 7.6 Hz, 1H), 7.20 (d, J = 7.9 Hz, 1H), 7.15 (m, 1H), 3.03 (m, 4H), 2.60 (s, 3H), 2.06 (s, 3H), 1.35 (m, 4H), 0.72 (m, 6H).

***N*-Ethyl-4-(5-(isopropylcarbamoyl)-2-methylphenylamino)-5-methylpyrrolo[1,2-*f*][1,2,4]triazine-6-carboxamide (7e).** This compound was prepared as a TFA salt in a similar way as **7i** was yield 20%, 98% purity by HPLC. LCMS (EI) m/z Calcd for $C_{21}H_{26}N_6O_2$ ($M + H$)⁺ = 395.21. Found: 395.21. ¹H NMR (400 MHz, MeOD) δ 7.91 (s, 1H), 7.77 (s, 1H), 7.67 (d, J = 8.0 Hz, 1H), 7.59 (s, 1H), 7.37 (d, J = 8.0 Hz, 1H), 4.11 (m, 1H), 3.30 (q, J = 7.3 Hz, 2H), 2.76 (s, 3H), 2.25 (s, 3H), 1.15 (d, J = 6.7 Hz, 6H), 1.14 (t, J = 7.3 Hz, 3H).

4-(5-(Butylcarbamoyl)-2-methylphenylamino)-*N*-ethyl-5-methylpyrrolo[1,2-*f*][1,2,4]triazine-6-carboxamide (7f). To a solution of 4-(5-(ethylcarbamoyl)-2-methylphenylamino)-5-methylpyrrolo[1,2-*f*][1,2,4]triazine-6-carboxylic acid (**8a**) (80 mg, 0.225 mmol) and *n*-butylamine (44 μ L, 0.45 mmol) in DMF (0.7 mL) was added HATU (68 mg, 0.27 mmol), and the resulting solution was stirred for 2 h. At this time, additional HATU (68 mg, 0.27 mmol) was added, and the mixture was allowed to stir at rt for an additional 1 h. The resulting mixture was then added dropwise into water (2.0 mL) with stirring. The solids were dispersed by sonicating for 1 min, and the suspension was stirred at rt for 1 h. The solid was collected by suction filtration and dried to afford the title compound (70 mg, 76% yield) as a white powder; 98% purity by HPLC. LCMS (EI) m/z Calcd for $C_{22}H_{28}N_6O_2$ ($M + H$)⁺ = 409.23. Found: 409.28. ¹H NMR (500 MHz, DMSO-*d*₆) δ 8.67 (s, 1H), 8.40 (t, J = 5.6 Hz, 1H), 8.11 (s, 1H), 8.09 (m, 1H), 7.94 (s, 1H), 7.79 (s, 1H), 7.72 (d, J = 8.0 Hz, 1H), 7.38 (d, J = 8.0 Hz, 1H), 3.30–3.24 (m, 4H), 2.83 (s, 3H), 2.25 (s, 3H), 1.51 (m, 2H), 1.33 (m, 2H), 1.13 (t, J = 7.2 Hz, 3H), 0.90 (t, J = 7.4 Hz, 3H).

***N*-Ethyl-4-(5-(2-methoxyethylcarbamoyl)-2-methylphenylamino)-5-methylpyrrolo[1,2-*f*][1,2,4]triazine-6-carboxamide (7g).** To a solution of 3-(6-(ethylcarbamoyl)-5-methylpyrrolo[1,2-*f*][1,2,4]triazin-4-ylamino)-4-methylbenzoic acid (**8a**) (19 mg, 0.054 mmol) in DMF (0.4 mL) was added HOBt (8 mg, 0.06 mmol) and EDC (11.5 mg, 0.06 mmol). The mixture was stirred at rt for 1 h before 2-methoxyethanamine (4.5 mg, 0.06 mmol) and DIPEA (14 mg, 0.11 mmol) were added. After stirring at rt for 16 h, the mixture was subjected to reverse-phase preparative HPLC to obtain the TFA salt of the title compound (14.0 mg, 49%) as a white solid; 98% purity by HPLC. LCMS (EI) m/z Calcd for $C_{21}H_{26}N_6O_3$ ($M + H$)⁺ = 411.21. Found: 211.20. ¹H NMR (500 MHz, MeOD) δ 8.28 (s, 1H), 7.97 (d, J = 7.7 Hz, 1H), 7.95 (s, 1H), 7.84 (s, 1H), 7.63 (d, J = 7.7 Hz, 1H), 3.57 (s, 3H), 3.41 (q, J = 7.3 Hz, 2H), 3.30 (m, 2H), 2.91 (s, 3H), 2.70 (br s, 2H), 2.42 (s, 3H), 1.24 (t, J = 7.3 Hz, 3H).

4-(5-(Cyclopropylcarbamoyl)-2-methylphenylamino)-*N*-ethyl-5-methylpyrrolo[1,2-*f*][1,2,4]triazine-6-carboxamide (7h). A mixture of 3-(6-(ethylcarbamoyl)-5-methylpyrrolo[1,2-*f*][1,2,4]triazin-4-ylamino)-4-methylbenzoic acid (**8a**) (0.936 g, 2.65 mmol), cyclopropylamine (0.360 mL, 5.20 mmol), EDC (0.635 g, 3.31 mmol), and 4-(dimethylamino)pyridine (65 mg, 0.532 mmol) in DMF (7 mL) was stirred at 45 °C for 20 h. The mixture was diluted with ethyl acetate (120 mL), washed sequentially with water (2 \times 25 mL), 10% aqueous Na₂CO₃ solution (25 mL), and brine (25 mL). The organic solution was dried over anhydrous MgSO₄ and concentrated under vacuum. The residue was subjected to flash chromatography (silica gel, 10% MeOH/CHCl₃) to provide the title product (0.448 g, 43% yield) as a white solid; 100% purity by HPLC. LCMS (EI) m/z Calcd for

$C_{21}H_{24}N_6O_2$ ($M + H$)⁺ = 393.20. Found: 393.33. ¹H NMR (500 MHz, DMSO-*d*₆) δ 8.31 (s, 1H), 8.23 (s, 1H), 7.93 (s, 1H), 7.92 (s, 1H), 7.70 (s, 1H), 7.57–7.54 (m, 2H), 7.28 (d, J = 7.8 Hz, 1H), 3.25 (m, 2H), 2.85 (m, 1H), 2.78 (s, 3H), 2.18 (s, 3H), 1.12 (t, J = 7.2 Hz, 3H), 0.68 (m, 2H), 0.57 (m, 2H).

4-(5-(Cyclobutylcarbamoyl)-2-methylphenylamino)-*N*-ethyl-5-methylpyrrolo[1,2-*f*][1,2,4]triazine-6-carboxamide (7i). This compound was prepared as a TFA salt in a similar way as **7i** was; Yield: 6.4%; 100% purity by HPLC. LCMS (EI) m/z Calcd for $C_{22}H_{26}N_6O_2$ ($M + H$)⁺ = 407.21. Found: 407.19. ¹H NMR (500 MHz, DMSO-*d*₆) δ 8.76 (br s, 1H), 8.62 (br s, 1H), 8.18–8.08 (m, 2H), 7.98 (br s, 1H), 7.87–7.73 (m, 2H), 7.43 (d, J = 7.5 Hz, 1H), 4.48 (m, 1H), 3.31 (m, 2H), 2.86 (s, 3H), 2.28 (s, 3H), 2.27–2.24 (m, 2H), 2.14 (m, 2H), 1.71 (m, 2H), 1.18 (t, J = 7.2 Hz, 3H).

4-(5-(Cyclopropylcarbamoyl)-2-methylphenylamino)-*N*,5-dimethylpyrrolo[1,2-*f*][1,2,4]triazine-6-carboxamide (7j). A mixture of 4-(5-(cyclopropylcarbamoyl)-2-methylphenylamino)-5-methylpyrrolo[1,2-*f*][1,2,4]triazine-6-carboxylic acid (**6b**) (0.026 g, 0.071 mmol), EDC (0.021 g, 0.11 mmol), HOBt (0.015 g, 0.11 mmol), methylamine hydrochloride (8.0 mg, 0.12 mmol), and diisopropylethylamine (0.040 mL, 0.23 mmol) in dimethylformamide (0.20 mL) was mechanically shaken at rt overnight. Water (1 mL) was added, and the precipitated material was collected by filtration, washed with water, and dried to give the title compound (0.019 g, 72% yield) as a white solid; 100% purity by HPLC. LCMS (EI) m/z Calcd for $C_{20}H_{22}N_6O_2$ ($M + H$)⁺ = 379.18. Found: 379.17. ¹H NMR (500 MHz, DMSO-*d*₆) δ 8.72 (s, 1H), 8.44 (d, J = 4.4 Hz, 1H), 8.12–8.11 (m, 2H), 7.96 (s, 1H), 7.84 (s, 1H), 7.75 (d, J = 8.0 Hz, 1H), 7.43 (d, J = 8.0 Hz, 1H), 2.92 (m, 1H), 2.87 (s, 3H), 2.81 (d, J = 4.4 Hz, 3H), 2.29 (s, 3H), 0.75 (m, 2H), 0.63 (m, 2H).

4-(5-(Cyclopropylcarbamoyl)-2-methylphenylamino)-5-methyl-*N*-propylpyrrolo[1,2-*f*][1,2,4]triazine-6-carboxamide (7k). A mixture of 4-(5-(cyclopropylcarbamoyl)-2-methylphenylamino)-5-methylpyrrolo[1,2-*f*][1,2,4]triazine-6-carboxylic acid (**6b**) (2.16 g, 5.91 mmol), *n*-propylamine (1.0 mL, 12.2 mmol), BOP (3.40 g, 7.69 mmol), and *N*-methylmorpholine (2.5 mL, 22.7 mmol) in DMF (10 mL) was stirred at 50 °C for 3 h. The mixture was poured into a mixture prepared from saturated NaHCO₃ solution (60 mL) and water (60 mL). The precipitating product was collected by suction filtration was washed with water. This crude product was suspended into ethyl acetate (100 mL) and stirred at 70 °C for 1 h. Upon cooling to rt, the title compound (2.07 g, 86% yield) was collected as a white solid by suction filtration; 98% purity by HPLC. LCMS (EI) m/z Calcd for $C_{22}H_{26}N_6O_2$ ($M + H$)⁺ = 407.21. Found: 407.22. ¹H NMR (500 MHz, DMSO-*d*₆) δ 8.49 (d, J = 3.6 Hz, 1H), 8.23 (s, 1H), 8.21 (s, 1H), 7.86 (s, 1H), 7.80 (s, 1H), 7.77 (d, J = 7.8 Hz, 1H), 7.42 (d, J = 7.8 Hz, 1H), 3.20 (m, 2H), 2.87 (m, 1H), 2.82 (s, 3H), 2.25 (s, 3H), 1.54 (m, 2H), 0.91 (t, J = 7.4 Hz, 3H), 0.68 (m, 2H), 0.59 (m, 2H). ¹³C NMR (125 MHz, DMSO-*d*₆) δ 167.3, 164.45, 155.3, 148.7, 138.8, 137.1, 133.0, 130.6, 127.2, 125.8, 119.6, 118.8, 114.4, 113.3, 41.0, 23.6, 23.1, 18.5, 12.1, 12.0, 6.2.

***N*-Butyl-4-(5-(cyclopropylcarbamoyl)-2-methylphenylamino)-5-methylpyrrolo[1,2-*f*][1,2,4]triazine-6-carboxamide (7l).** A mixture of 4-(5-(cyclopropylcarbamoyl)-2-methylphenylamino)-5-methylpyrrolo[1,2-*f*][1,2,4]triazine-6-carboxylic acid (**6b**) (0.026 g, 0.071 mmol), EDC (0.021 g, 0.11 mmol), HOBt (0.015 g, 0.11 mmol), *n*-butylamine (0.015 mL, 0.15 mmol), and diisopropylethylamine (0.040 mL, 0.23 mmol) in dimethylformamide (0.20 mL) was mechanically shaken at rt overnight. Water (1 mL) was added, and the precipitated material was collected by filtration, washed with water, and dried to give the title compound (0.021 g, 70% yield) as a white solid; 98% purity by HPLC. LCMS (EI) m/z Calcd for $C_{23}H_{28}N_6O_2$ ($M + H$)⁺ = 421.23. Found: 421.18. ¹H NMR (500 MHz, DMSO-*d*₆) δ 8.72 (s, 1H), 8.46 (d, J = 4.2 Hz, 1H), 8.16 (s, 1H), 8.11 (t, J = 5.7 Hz, 1H), 7.96 (s, 1H), 7.84 (s, 1H), 7.75 (d, J = 8.0 Hz, 1H), 7.43 (d, J = 8.0 Hz, 1H), 3.28 (m, 2H), 2.92 (m, 1H), 2.87 (s, 3H), 2.29 (s, 3H), 1.56 (m, 2H), 1.41 (m, 2H), 0.98 (t, J = 7.4 Hz, 3H), 0.74 (m, 2H), 0.63 (m, 2H).

(**S**)-4-(5-(Cyclopropylcarbamoyl)-2-methylphenylamino)-5-methyl-*N*-(1-phenylethyl)pyrrolo[1,2-*f*][1,2,4]triazine-6-carboxamide (**7m**). A mixture of (**S**)-4-methyl-3-(5-methyl-6-(1-phenylethylcarbamoyl)pyrrolo[1,2-*f*][1,2,4]triazin-4-ylamino)benzoic acid (**8b**) (34.4 mg, 0.080 mmol), cyclopropylamine (0.010 mL, 0.144 mmol), 1-(3-dimethylaminopropyl)-3-ethylcarbodiimide hydrochloride (EDC) (20.1 mg, 0.104 mmol), and *N,N*-dimethylpyridin-4-amine (DMAP) (2.4 mg, 0.020 mmol) in DMF (0.5 mL) was stirred at rt for 16 h. The reaction mixture was diluted with methanol (1.5 mL) and injected to prep. HPLC to afford the title compound (30.2 mg, 81% yield) as a white solid; 100% purity by HPLC. LCMS (EI) *m/z* Calcd for $C_{27}H_{28}N_6O_2$ ($M + H$)⁺ = 469.23. Found: 469.35. ¹H NMR (500 MHz, DMSO-*d*₆) δ 8.59 (s, 1H), 5.06 (m, 1H), 8.37 (d, *J* = 8.0 Hz, 1H), 8.32 (d, *J* = 4.2 Hz, 1H), 8.20 (s, 1H), 7.82 (s, 1H), 7.72 (s, 1H), 7.61 (d, *J* = 7.7 Hz, 1H), 7.32–7.23 (m, 5H), 7.14 (m, 1H), 2.76 (m, 1H), 2.70 (s, 3H), 2.14 (s, 3H), 1.38 (d, *J* = 7.2 Hz, 3H), 0.59 (m, 2H), 0.48 (m, 2H).

(**S**)-*N*-sec-Butyl-4-(5-(cyclopropylcarbamoyl)-2-methylphenylamino)-5-methylpyrrolo[1,2-*f*][1,2,4]triazine-6-carboxamide (**7n**). This compound was prepared in the same way as **7l**; Yield: 76%; 100% purity by HPLC. LCMS (EI) *m/z* Calcd for $C_{23}H_{28}N_6O_2$ ($M + H$)⁺ = 421.23. Found: 421.22. ¹H NMR (500 MHz, DMSO-*d*₆) δ 8.72 (s, 1H), 8.46 (s, 1H), 8.22 (s, 1H), 7.98 (s, 1H), 7.86 (s, 1H), 7.83 (s, 1H), 7.76 (d, *J* = 8.0 Hz, 1H), 7.44 (d, *J* = 8.0 Hz, 1H), 3.97 (m, 1H), 2.93 (m, 1H), 2.88 (s, 3H), 2.30 (s, 3H), 1.56 (m, 2H), 1.20 (d, *J* = 6.7 Hz, 3H), 0.96 (t, *J* = 7.4 Hz, 3H), 0.76 (m, 2H), 0.64 (m, 2H).

4-(5-(Cyclopropylcarbamoyl)-2-methylphenylamino)-*N*-(2-methoxyethyl)-5-methylpyrrolo[1,2-*f*][1,2,4]triazine-6-carboxamide (**7o**). This compound was prepared in the same way as **7l**; Yield: 73%; 100% purity by HPLC. LCMS (EI) *m/z* Calcd for $C_{22}H_{26}N_6O_2$ ($M + H$)⁺ = 423.21. Found: 423.17. ¹H NMR (500 MHz, DMSO-*d*₆) δ 8.73 (s, 1H), 8.46 (d, *J* = 4.4 Hz, 1H), 8.22 (t, *J* = 5.4 Hz, 1H), 8.20 (s, 1H), 7.96 (s, 1H), 7.85 (s, 1H), 7.75 (d, *J* = 8.0 Hz, 1H), 7.43 (d, *J* = 8.0 Hz, 1H), 3.51 (m, 2H), 3.46 (m, 2H), 3.38 (s, 3H), 2.92 (m, 1H), 2.88 (s, 3H), 2.29 (s, 3H), 0.75 (m, 2H), 0.63 (m, 2H).

(**R**)-4-(5-(Cyclopropylcarbamoyl)-2-methylphenylamino)-*N*-(2-hydroxy-1-phenylethyl)-5-methylpyrrolo[1,2-*f*][1,2,4]triazine-6-carboxamide (**7p**). This compound was prepared in the same way as **7l**; Yield: 59%; 100% purity by HPLC. LCMS (EI) *m/z* Calcd for $C_{27}H_{28}N_6O_3$ ($M + H$)⁺ = 485.22. Found: 485.92. ¹H NMR (500 MHz, DMSO-*d*₆) δ 8.73 (s, 1H), 8.46 (d, *J* = 4.4 Hz, 1H), 8.41 (d, *J* = 8.2 Hz, 1H), 8.39 (s, 1H), 7.97 (s, 1H), 7.87 (s, 1H), 7.75 (d, *J* = 7.7 Hz), 7.47–7.37 (m, 5H), 7.30 (m, 1H), 5.11 (m, 1H), 5.00 (m, 1H), 3.72 (m, 2H), 2.92 (m, 1H), 2.85 (s, 3H), 2.29 (s, 3H), 0.74 (m, 2H), 0.63 (m, 2H).

(**S**)-5-Methyl-4-(2-methyl-5-(phenylcarbamoyl)phenylamino)-*N*-(1-phenylethyl)-pyrrolo[1,2-*f*][1,2,4]triazine-6-carboxamide (**7q**). To a solution of (**S**)-4-methyl-3-(5-methyl-6-(1-phenylethylcarbamoyl)pyrrolo[1,2-*f*][1,2,4]triazin-4-ylamino)benzoic acid (**8b**) (50 mg, 0.116 mmol) in DMF (0.3 mL) were successively added diisopropylethylamine (61 μL, 0.348 mmol) and HATU (66 mg, 0.174 mmol). The resulting solution was stirred at rt for 20 min before aniline (21 μL, 0.232 mmol) was added. The mixture was heated at 70 °C for 15 h, then subjected to preparative HPLC to afford the title compound (2.0 mg, 3% yield) as a tan solid; 98% purity by HPLC. LCMS (EI) *m/z* Calcd for $C_{30}H_{28}N_6O_2$ ($M + H$)⁺ = 505.23. Found: 505.30.

N-Ethyl-5-methyl-4-(2-methyl-5-(thiazol-2-ylcarbamoyl)phenylamino)pyrrolo[1,2-*f*][1,2,4]triazine-6-carboxamide (**7r**). A mixture of 3-(6-(ethylcarbamoyl)-5-methylpyrrolo[1,2-*f*][1,2,4]triazin-4-ylamino)-4-methylbenzoic acid (**8a**) (97.2 mg, 0.275 mmol), 2-aminothiazole (42.7 mg, 0.426 mmol), benzotriazole-1-yl-oxy-tris(dimethylamino)phosphonium hexafluorophosphate (BOP) (250 mg, 0.565 mmol), and *N*-methylmorpholine (0.15 mL, 1.36 mmol) in DMF (1 mL) was heated at 55 °C for 16 h. The mixture was diluted with ethyl acetate, washed sequentially with water, saturated NaHCO₃ solution, and brine. The organic solution was dried over anhydrous MgSO₄ and concentrated under vacuum.

The residue was subjected to preparative HPLC to provide the desired product (36.4 mg, 30% yield) as an off-white solid; 100% purity by HPLC. LCMS (EI) *m/z* Calcd for $C_{21}H_{21}N_7O_2S$ ($M + H$)⁺ = 436.15. Found: 436.36. ¹H NMR (500 MHz, DMSO-*d*₆) δ 12.52 (s, 1H), 8.59 (s, 1H), 8.17 (s, 1H), 8.04 (s, 1H), 8.02 (t, *J* = 5.6 Hz, 1H), 7.90 (d, *J* = 8.0 Hz, 1H), 7.74 (s, 1H), 7.48 (d, *J* = 3.2 Hz, 1H), 7.39 (d, *J* = 8.0 Hz, 1H), 7.20 (d, *J* = 3.2 Hz, 1H), 3.18 (m, 2H), 2.76 (s, 3H), 2.22 (s, 3H), 1.04 (t, *J* = 7.2 Hz, 3H).

N-Ethyl-5-methyl-4-(2-methyl-5-(5-methylthiazol-2-ylcarbamoyl)phenylamino)pyrrolo[1,2-*f*][1,2,4]triazine-6-carboxamide (**7s**). This compound was prepared in the same way as **7r**; yield 71%; 100% purity by HPLC. LCMS (EI) *m/z* Calcd for $C_{22}H_{23}N_7O_2S$ ($M + H$)⁺ = 450.16. Found: 450.19. ¹H NMR (500 MHz, DMSO-*d*₆/D₂O) δ ppm 8.12 (s, 1H), 8.02 (s, 1H), 7.87 (d, *J* = 7.2 Hz, 1H), 7.75 (s, 1H), 7.42 (d, *J* = 8.05 Hz, 1H), 7.15 (s, 1H), 3.20 (q, *J* = 7.2 Hz, 2H), 2.76 (s, 3H), 2.31 (s, 3H), 2.23 (s, 3H), 1.07 (t, *J* = 7.21 Hz, 3H).

N-Ethyl-5-methyl-4-(2-methyl-5-(oxazol-2-ylcarbamoyl)phenylamino)pyrrolo[1,2-*f*][1,2,4]triazine-6-carboxamide (**7t**). A mixture of 3-(6-(ethylcarbamoyl)-5-methylpyrrolo[1,2-*f*][1,2,4]triazin-4-ylamino)-4-methylbenzoic acid (**8a**) (120 mg, 0.306 mmol), 2-aminooxazole (103 mg, 1.22 mmol), BOP (271 mg, 0.613 mmol), and *N*-methylmorpholine (0.20 mL, 1.80 mmol) in DMF (1 mL) was heated at 70 °C for 16 h. The mixture was diluted with ethyl acetate (60 mL), and washed sequentially with water, saturated NaHCO₃ solution, and brine. The organic solution was dried over anhydrous MgSO₄ and concentrated under vacuum. The residue was subjected to flash chromatography (silica gel, 8% MeOH/CHCl₃) to provide the desired product (53 mg, 41% yield) as beige solid; 100% purity by HPLC. LCMS (EI) *m/z* Calcd for $C_{21}H_{21}N_7O_3$ ($M + H$)⁺ = 420.17. Found: 420.25. ¹H NMR (500 MHz, DMSO-*d*₆/D₂O) δ 8.22 (s, 1H), 8.15 (s, 1H), 8.00 (s, 1H), 7.91 (d, *J* = 7.4 Hz, 1H), 7.87 (s, 1H), 7.54 (d, *J* = 7.4 Hz, 1H), 7.25 (s, 1H), 3.33 (q, *J* = 7.2 Hz, 2H), 2.88 (s, 3H), 2.35 (s, 3H), 1.19 (t, *J* = 7.2 Hz, 3H).

N-Ethyl-4-(5-(isoxazol-3-ylcarbamoyl)-2-methylphenylamino)-5-methylpyrrolo[1,2-*f*][1,2,4]triazine-6-carboxamide (**7u**). A mixture of 3-(6-(ethylcarbamoyl)-5-methylpyrrolo[1,2-*f*][1,2,4]triazin-4-ylamino)-4-methylbenzoic acid (**8a**) (12.0 g, 34.0 mmol), 3-aminoisoxazole (12.5 mL, 169 mmol), BOP (30.1 g, 68.0 mmol), and *N*-methylmorpholine (22.4 mL, 204 mmol) in DMF (100 mL) was heated at 65 °C for 48 h. The mixture was concentrated under vacuum to approximately two-thirds of its original volume and then poured into saturated NaHCO₃ solution (900 mL). The precipitating product was collected by suction filtration and dried over Drierite under vacuum. The crude product was subjected to flash chromatography (silica gel, 5% MeOH/CHCl₃). The correct fractions were combined and concentrated to a volume of approximately 100 mL. The insoluble product (3.38 g, 24%) was collected as a white solid by suction filtration; 100% purity by HPLC. LCMS (EI) *m/z* Calcd for $C_{21}H_{21}N_7O_3$ ($M + H$)⁺ = 420.17. Found: 420.20. ¹H NMR (500 MHz, DMSO-*d*₆) δ 11.4 (s, 1H), 8.86 (s, 1H), 8.69 (s, 1H), 8.18 (s, 1H), 8.12 (s, 1H), 8.11 (t, *J* = 5.5 Hz, 1H), 7.93 (d, *J* = 8.0 Hz, 1H), 7.83 (s, 1H), 7.47 (d, *J* = 8.0 Hz, 1H), 7.06 (s, 1H), 3.27 (m, 2H), 2.84 (s, 3H), 2.30 (s, 3H), 1.13 (t, *J* = 7.2 Hz, 3H).

4-(5-(Isioxazol-3-ylcarbamoyl)-2-methylphenylamino)-5-methyl-*N*-propylpyrrolo[1,2-*f*][1,2,4]triazine-6-carboxamide (**7v**). This compound was prepared in a similar way from **8c** as **7u** was from **8a**; yield 20%; 99% purity by HPLC. LCMS (EI) *m/z* Calcd for $C_{22}H_{23}N_7O_3$ ($M + H$)⁺ = 420.19. Found: 434.29. ¹H NMR (500 MHz, DMSO-*d*₆) δ 11.4 (s, 1H), 8.86 (s, 1H), 8.68 (s, 1H), 8.18 (s, 1H), 8.13 (s, 1H), 8.09 (t, *J* = 5.6 Hz, 1H), 7.92 (d, *J* = 8.0 Hz, 1H), 7.82 (s, 1H), 7.47 (d, *J* = 8.0 Hz, 1H), 7.06 (s, 1H), 3.19 (m, 2H), 2.84 (s, 3H), 2.30 (s, 3H), 1.53 (m, 2H), 0.91 (t, *J* = 7.4 Hz, 3H).

p38α Kinase Assay. The assays were performed in V-bottomed 96-well plates. The final assay volume was 60 μL, which was from three 20 μL additions of enzyme, substrates (myelin basic protein (MBP) and ATP), and test compounds in assay buffer (50 mM Tris pH 7.5, 10 mM MgCl₂, 50 mM NaCl, and

1 mM DTT). Bacterially expressed, activated p38 was preincubated with test compounds for 10 min prior to the initiation of reaction by adding substrates. The plates were incubated at room temperature for 45 min. The reaction was terminated by adding 5 μ L of 0.5 M EDTA to each well. The reaction mixture was aspirated onto a prewet filter mat using a Skatron Micro96 cell harvester (Skatron) and washed with PBS. The filtermat was dried in a microwave oven for 1 min, coated with a layer of MeltillLex A scintillation wax (PerkinElmer), and counted on a Microbeta scintillation counter (model 1450, PerkinElmer). The data were analyzed using the Prism nonlinear least-squares regression (GraphPad Software). The final concentrations of reagents in the assays were [ATP], 1 μ M; [γ -³³P]ATP], 3 nM; [MBP] (Sigma, M1891), 2 μ g/well; [p38], 15 ng/well; [DMSO], 0.3%.

LPS-Induced TNF α Production in Human PBMC. Human PBMCs were isolated from whole blood collected from healthy donors. Blood was diluted into RPMI 1640 (Life Technologies) containing 2.5 mM EDTA (Life Technologies), 10 μ g/mL polymyxin (Sigma), and then underlaid with ficoll (Accurate Scientific Co.) and centrifuged at 600g for 25 min. The interface was collected and cells were washed twice and resuspended in RPMI, 10% FBS. Cells are then distributed (200 μ L/well) into 96-well tissue culture treated plates (Falcon) at 1×10^6 cells/mL in RPMI, 10% FBS. Test compounds were added to appropriate wells and incubated with cells for 30 min. Cells were then stimulated by the addition of lipopolysaccharide (LPS, BioWhittaker), with a final concentration of 25 ng/mL, and incubated for 6 h at 37 °C, 5% CO₂. The cell supernatants were removed and assayed for TNF α by ELISA (R&D Systems).

Inhibition of TNF α Release in Mice. BALB/c female mice, 6–8 weeks of age, were obtained from Harlan Laboratories and maintained ad libitum on water and standard rodent chow (Harlan Teklad). Mice were acclimated to ambient conditions for at least one week prior to use. For oral dosing, the compounds were prepared in a solution of 100% polyethylene glycol (mw 300) and a dosing volume of 0.2 mL per mouse was administered by gavage at various times (see Table 6) prior to LPS injection (0.5 mL of LPS suspended at 2 μ g/mL in PBS, administered ip). Blood samples were obtained 90 min after LPS injection. Serum was separated from clotted blood samples by centrifugation (5 min, 5000g, room temperature) and analyzed for levels of TNF α by ELISA assay (R&D Systems) according to the manufacturer's directions. Results are shown as mean \pm SD of $n = 8$ mice per treatment group. All procedures involving animals were reviewed and approved by the Institutional Animal Care and Use Committee.

Rat Adjuvant Arthritis. Male Lewis rats (Harlan, 175–200 g) were immunized sc at the base of the tail with 0.1 mL complete Freund's adjuvant containing 10 mg/mL *Mycobacterium butyricum*. Seven days later, baseline (predisease) measurements of hind paw volume were determined by volume displacement plethysmometry (Ugo Basile, Italy). Compounds were administered orally in 1 mL PEG 300 beginning on day 11. Paw volume measurements were repeated 3 times/week for the remainder of the study. Data are presented as the summed increase in volume (expressed in mL) above baseline for each rat's two hind paws.

Mouse Pharmacokinetic Study of 7k. Three groups of male BALB/c mice (20–25 g) were fasted overnight and received compound 7k as an intravenous (IV) bolus dose (5 mg/kg with 20% NMP, 35% PEG 400, 10% PG, and 35% water as a vehicle) or by oral gavage (10 mg/kg with PEG 400 as a vehicle). Blood samples (0.2 mL) were obtained retro-orbital bleeding at 0.05, 0.25, 0.5, 1, 3, 6, 8, and 24 h post dose for the IV group and at 0.25, 0.5, 1, 3, 6, 8, and 24 h post dose for the PO dose group. At each time point, three mice were bled, resulting in a composite pharmacokinetic profile. The tubes were inverted several times to ensure mixing and placed on ice. Plasma was obtained following centrifugation at 4 °C (1500–2000g). Plasma samples were stored at –20 °C until analysis by a nonchiral LC/MS/MS assay.

Rat Pharmacokinetic Study of 7k. Three groups of male Sprague–Dawley rats (250–300 g) were fasted overnight and received compound 7k as an intravenous (IV) bolus dose (2.5 mg/kg with 25% NMP, 33% PEG 400, 9% PG, and 33% water as a vehicle) or by oral gavage (10 mg/kg with PEG 400 as a vehicle). Blood samples (0.3 mL) were obtained retro-orbital bleeding at 0.05, 0.25, 0.5, 1, 3, 6, 8, and 24 h post dose for the IV group and at 0.25, 0.5, 1, 3, 6, 8, and 24 h post dose for the PO dose group. At each time point, three mice were bled resulting in a composite pharmacokinetic profile. The tubes were inverted several times to ensure mixing and placed on ice. Plasma was obtained following centrifugation at 4 °C (1500–2000g). Plasma samples were stored at –20 °C until analysis by a nonchiral LC/MS/MS assay.

Co-Crystal Structure of 7k and 7v with p38 MAP Kinase. His-p38 MAP kinase was expressed in *Escherichia coli* (BL21 DE3) and purified by sequential anion exchange, nickel chelate affinity, and size exclusion chromatography. The protein at 2 mg/mL, in 25 mM Tris (pH 7.4), 50 mM NaCl, 5% glycerol, 2 mM DTT, was complexed with a 5-fold molar excess of 7k or 7v and then concentrated to 17 mg/mL. Co-crystals were grown by the hanging drop method from solutions containing 30% PEG 10K, 5 mM MgSO₄, 50 mM MES, pH 6.0. Data were collected to approximately 2.2 Å resolution on the R-Axis IV area detector, reduced using the Denzo/HKL package, and refined by the method of simulated annealing using program CNX.

References

- (1) (a) Schieven, G. L. The biology of p38 kinase: A central role in inflammation. *Curr. Top. Med. Chem.* **2005**, *5*, 921–928. (b) Saklatvala, J. The p38 MAP kinase pathway as a therapeutic target in inflammatory disease. *Curr. Opin. Pharmacol.* **2004**, *4*, 372–377. (c) Kumar, S.; Borhm, J.; Lee, J. C. P38 MAP Kinases: Key Signaling Molecules as Therapeutic Targets for Inflammatory Diseases. *Nature Rev. Drug Discovery* **2003**, *2*, 717–726. (d) Adams, J. L.; Badge, A. M.; Kumar, S.; Lee, J. C. p38 MAP kinase: molecular target for the inhibition of pro-inflammatory cytokines. *Prog. Med. Chem.* **2001**, *38*, 1–60. (e) Herlaar, E.; Brown, Z. p38 MAPK signaling cascades in inflammatory disease. *Mol. Med. Today* **1999**, *5*, 439–447. (f) Lee, J. C.; Laydon, J. T.; McDonnell, P. C.; Gallagher, T. F.; Kimar, S.; Green, D.; McNulty, D.; Blumenthal, M. J.; Heys, J. R.; Landvatter, S. W.; Strickler, J. E.; McLaughlin, M. M.; Siemens, I. R.; Fisher, S. M.; Livy, G. P.; White, J. R.; Adams, J. L.; Young, P. R. A protein kinase involved in the regulation of inflammatory cytokine biosynthesis. *Nature* **1994**, *372*, 739–745.
- (2) For example, (a) Pettus, L. H.; Wurz, R. P.; Xu, S.; Herberich, B.; Henkle, B.; Liu, Q.; McBride, H. J.; Mu, S.; Plant, M. H.; Saris, C. J. M.; Sherman, L.; Wong, L. M.; Chmait, S.; Lee, M. R.; Mohr, C.; Hsieh, F.; Tasker, A. S. Discovery and Evaluation of 7-Alkyl-1,5-bis-aryl-pyrazolopyridinones as Highly Potent, Selective, and Orally Efficacious Inhibitors of p38 α Mitogen-Activated Protein Kinase. *J. Med. Chem.* **2010**, *53*, 2973–2985. (b) Selness, S. R.; Devraj, R. V.; Monahan, J. B.; Boehm, T. L.; Walker, J. K.; Devadas, B.; Durley, R. C.; Kurumbail, R.; Shieh, H.; Xing, L.; Hepperle, M.; Rucker, P. V.; Jerome, K. D.; Benson, A. G.; Marrufo, L. D.; Madsen, H. M.; Hitchcock, J.; Owen, T. J.; Christie, L.; Promo, M. A.; Hickory, B. S.; Alvira, E.; Naing, W.; Blevis-Bal, R. Discovery of N-substituted pyridinones as potent and selective inhibitors of p38 kinase. *Bioorg. Med. Chem. Lett.* **2009**, *19*, 5852–5856. (c) Herberich, B.; Cao, G.-Q.; Chakrabarti, P. P.; Falsey, J. R.; Pettus, L.; Rzas, R. M.; Reed, A. B.; Reichelt, A.; Sham, K.; Thaman, M.; Wurz, R. P.; Xu, S.; Zhang, D.; Hsieh, F.; Lee, M. R.; Syed, R.; Li, V.; Grosfeld, D.; Plant, M. H.; Henkle, B.; Sherman, L.; Middleton, S.; Wong, L. M.; Tasker, A. S. Discovery of Highly Selective and Potent p38 Inhibitors Based on a Phthalazine Scaffold. *J. Med. Chem.* **2008**, *51*, 6271–6279. (d) Natarajan, S. R.; Liu, L.; Levorse, M.; Thompson, J. E.; O'Neill, E. A.; O'Keefe, S. J.; Vora, K. A.; Cvetovich, R.; Chung, J. Y.; Carballo-Jane, E.; Visco, D. M. p38 MAP kinase inhibitors. Discovery of an orally bioavailable and highly efficacious compound based on the 7-amino-naphthyridone scaffold. *Bioorg. Med. Chem. Lett.* **2006**, *16*, 5468–5471. (e) McClure, K. F.; Letavic, M. A.; Kalgutkar, A. S.; Gabel, C. A.; Audoly, L.; Barberia, J. T.; Braganza, J. F.; Carter, D.; Carty, T. J.; Cortina, S. R.; Dombroski, M. A.; Donahue, K. M.; Elliott, N. C.; Gibbons, C. P.; Jordan, C. K.; Kuperman, A. V.; Labasi, J. M.; LaLiberte, R. E.; McCoy, J. M.; Naiman, B. M.; Nelson, K. L.; Nguyen, H. T.; Peese, K. M.; Sweeney, F. J.; Taylor, T. J.; Trebino, C. E.;

- Abramov, Y. A.; Laird, E. R.; Volberg, W. A.; Zhou, J.; Bach, J.; Lombardo, F. Structure–activity relationships of triazolopyridine oxazole p38 inhibitors: identification of candidates for clinical development. *Bioorg. Med. Chem. Lett.* **2006**, *16*, 4339–4344. (f) Liu, C.; Wroblewski, S. T.; Lin, J.; Gillooly, K. M.; McIntyre, K.; Pitt, S.; Shen, D. R.; Shuster, D. J.; Zhang, H.; Doweiko, A. M.; Sack, J. S.; Barrish, J. C.; Dodd, J. H.; Schieven, G. L.; Leftheris, K. 5-Cyanopyrimidine Derivatives as a Novel Class of Potent, Selective, and Orally Active Inhibitors of p38 α MAP Kinase. *J. Med. Chem.* **2005**, *48*, 6261–6270. (g) Revesz, L.; Blum, E.; Di Padova, F. E.; Buhl, T.; Feifel, R.; Gram, H.; Hiestand, P.; Manning, U.; Rucklin, G. Novel p38 inhibitors with potent oral efficacy in several models of rheumatoid arthritis. *Bioorg. Med. Chem. Lett.* **2004**, *14*, 3595–99. (h) Trejo, A.; Arzeno, H.; Browner, M.; Chanda, S.; Cheng, S.; Comer, D. D.; Dalrymple, S. A.; Dunten, P.; Lafargue, J.; Lovejoy, B.; Freire-Moar, J.; Lim, J.; McIntosh, J.; Miller, J.; Papp, E.; Reuter, D.; Roberts, R.; Saunders, J.; Song, K.; Villaseñor, A.; Warren, S. D.; Welch, M.; Weller, P.; Whiteley, P. E.; Zeng, Lu; Goldstein, D. M. Design and synthesis of 4-azaindoles as inhibitors of p38 MAP kinase. *J. Med. Chem.* **2003**, *46*, 4702–4713. (i) Rupert, K. C.; Henry, J. R.; Dodd, J. H.; Wadsworth, S. A.; Cavender, D. E.; Olini, G. C.; Fahmy, B.; Siekierka, J. J. Imidazopyrimidines, potent inhibitors of p38 MAP kinase. *Bioorg. Med. Chem. Lett.* **2003**, *13*, 347–350. (j) Regan, J.; Breitfelder, S.; Cirillo, P.; Gilmore, T.; Graham, A. G.; Hickey, E.; Klaus, B.; Madwed, J.; Moriak, M.; Moss, N.; Pargellis, C.; Pav, S.; Proto, A.; Swinamer, A.; Tong, L.; Torcellini, C. Pyrazole urea-based inhibitors of p38 MAP kinase: From lead compound to clinical candidate. *J. Med. Chem.* **2002**, *45*, 2994–3008.
- (3) (a) Choy, E. H. S.; Panayi, G. S. Cytokine Pathway and Joint Inflammation in Rheumatoid Arthritis. *N. Engl. J. Med.* **2001**, *344*, 907–916. (b) Foster, M. L.; Halley, F.; Souness, J. E. Potential of p38 inhibitors in the treatment of rheumatoid arthritis. *Drug News Perspect.* **2000**, *13*, 488–497. (c) Feldmann, M.; Brennan, F. M.; Maini, R. N. Role of cytokines in rheumatoid arthritis. *Annu. Rev. Immunol.* **1996**, *14*, 397–440. (d) Dinarello, C. A. Inflammatory cytokines: Interleukin-1 and Tumor Necrosis Factor as Effector Molecules in Autoimmune Diseases. *Curr. Opin. Immunol.* **1991**, *3*, 941–948.
- (4) (a) Jarvis, B.; Faulds, D. Etanercept: a review of its use in rheumatoid arthritis. *Drugs* **1999**, *57*, 945–966. (b) Rutgeerts, P. J. Review article: efficacy of infliximab in Crohn's disease—induction and maintenance of remission. *Aliment. Pharmacol. Ther.* **1999**, *13* (Suppl 4), 9–15.
- (5) (a) Sweeney, S. E. The as-yet unfulfilled promise of p38 MAPK inhibitors. *Nature Rev. Rheumatol.* **2009**, *5*, 475–477. (b) Karcher, S. C.; Laufer, S. A. Successful structure-based design of recent p38 MAP kinase inhibitors. *Curr. Top. Med. Chem.* **2009**, *9*, 655–676. (c) Pettus, L. H.; Wurz, R. P. Small molecule p38 MAP kinase inhibitors for the treatment of inflammatory diseases: novel structures and developments during 2006–2008. *Curr. Top. Med. Chem.* **2008**, *8*, 1452–1467. (d) Goldstein, D. M.; Gabriel, T. Pathway to the clinic: Inhibition of p38 MAP kinase. A review of ten chemotypes selected for development. *Curr. Top. Med. Chem.* **2005**, *5*, 1017–1029. (e) Wroblewski, S. T.; Doweiko, A. M. Structural comparison of p38 inhibitor–protein complexes: a review of recent p38 inhibitors having unique binding interactions. *Curr. Top. Med. Chem.* **2005**, *5*, 1005–1016. (f) Natarajan, S. R.; Doherty, J. B. P38 MAP kinase inhibitors: Evolution of imidazole-based and pyrido-pyrimidin-2-one lead classes. *Curr. Top. Med. Chem.* **2005**, *5*, 987–1003. (g) Hynes, J.; Leftheris, K. Small molecule p38 inhibitors: novel structural features and advances from 2002–2005. *Curr. Top. Med. Chem.* **2005**, *5*, 967–985. (h) Diller, D. J.; Lin, T. H.; Metzger, A. The discovery of novel chemotypes of p38 kinase inhibitors. *Curr. Top. Med. Chem.* **2005**, *5*, 953–965. (i) Bolós, J. Structure–activity relationships of p38 mitogen-activated protein kinase inhibitors. *Mini-Rev. Med. Chem.* **2005**, *5*, 857–868. (j) Dominguez, C.; Powers, D. A.; Tamayo, N. p38 MAP kinase inhibitors: Many are made, but few are chosen. *Curr. Opin Drug Discovery Dev.* **2005**, *8* (4), 421–430.
- (6) Ding, C. Drug evaluation: VX-702, a MAP kinase inhibitor for rheumatoid arthritis and acute coronary syndrome. *Curr. Opin. Invest. Drugs* **2006**, *7* (11), 1020–1025.
- (7) Goldstein, D. M.; Kuglstat, A.; Lou, Y.; Soth, M. J. Selective p38 α Inhibitors Clinically Evaluated for the Treatment of Chronic Inflammatory Disorders. *J. Med. Chem.* **2010**, *53*, 2345–2353.
- (8) Hill, R. J.; Dabbagh, K.; Phippard, D.; Li, C.; Suttman, R. T.; Welch, M.; Papp, E.; Song, K. W.; Chang, K.-C.; Leaffer, D.; Kim, Y.-N.; Roberts, R. T.; Zabka, T. S.; Aud, D.; Dal Porto, J.; Manning, A. M.; Peng, S. L.; Goldstein, D. M.; Wong, B. R. Pamapimod, a novel p38 mitogen-activated protein kinase inhibitor: preclinical analysis of efficacy and selectivity. *J. Pharmacol. Exp. Ther.* **2008**, *327* (3), 610–619.
- (9) Regan, J.; Capolino, A.; Cirillo, P. F.; Gilmore, T.; Graham, A. G.; Hickey, E.; Kroe, R. R.; Madwed, J.; Moriak, M.; Nelson, R.; Pargellis, C. A.; Swinamer, A.; Torcellini, C.; Tsang, M.; Moss, N. Structure–Activity Relationships of the p38 α MAP Kinase Inhibitor 1-(5-tert-Butyl-2-p-tolyl-2H-pyrazol-3-yl)-3-[4-(2-morpholin-4-yl-ethoxy)naphthalen-1-yl]urea (BIRB 796). *J. Med. Chem.* **2003**, *46* (22), 4676–4686.
- (10) Nikas, S. N.; Drosos, A. A. SCIO-469 (Scios Inc.). *Curr. Opin. Invest. Drugs* **2004**, *5* (11), 1205–1212.
- (11) Xing, Li; Shieh, H. S.; Selness, S. R.; Devraj, R. V.; Walker, J. K.; Devadas, B.; Hope, H. R.; Compton, R. P.; Schindler, J. F.; Hirsch, J. L.; Benson, A. G.; Kurumbail, R. G.; Stegeman, R. A.; Williams, J. M.; Broadus, R. M.; Walden, Z.; Monahan, J. B. Structure Bioinformatics-Based Prediction of Exceptional Selectivity of p38 MAP Kinase Inhibitor PH-797804. *Biochemistry* **2009**, *48*, 6402–6411.
- (12) Hynes, J., Jr.; Dyckman, A. J.; Lin, S.; Wroblewski, S.; Wu, H.; Gillooly, K. M.; Kanner, S. B.; Lonial, H.; Loo, D.; McIntyre, K. W.; Pitt, S.; Shen, D. R.; Shuster, D. J.; Yang, X.; Zhang, R.; Behnia, K.; Zhang, H.; Marathe, P. H.; Doweiko, A. M.; Tokarski, J. S.; Sack, J. S.; Pokross, M.; Kiefer, S. E.; Newitt, J. A.; Barrish, J. C.; Dodd, J. H.; Schieven, G. L.; Leftheris, K. Design, Synthesis, and Anti-inflammatory Properties of Orally Active 4-(Phenylamino)-pyrrolo[2,1-f][1,2,4]triazine p38 α Mitogen-Activated Protein Kinase Inhibitors. *J. Med. Chem.* **2008**, *51*, 4–16.
- (13) Wroblewski, S. T.; Lin, S.; Hynes, J.; Wu, H.; Pitt, S.; Shen, D. R.; Zhang, R.; Gillooly, K. M.; Shuster, D. J.; McIntyre, K. W.; Doweiko, A. M.; Kish, K. F.; Tredup, J. A.; Duke, G. J.; Sack, J. S.; McKinnon, M.; Dodd, J.; Barrish, J. C.; Schieven, G. L.; Leftheris, K. Synthesis and SAR of new pyrrolo[2,1-f][1,2,4]triazines as potent p38 α MAP kinase inhibitors. *Bioorg. Med. Chem. Lett.* **2008**, *18*, 2739–2744.
- (14) Cambanis, A.; Dobre, V.; Niculescu-Duvaz, I. Potential anticancer agents. V. Aromatic nitrogen mustards related to 3-[N,N-bis(2-chloroethyl)amino]-4-methylbenzoic acid. *J. Med. Chem.* **1969**, *12*, 161–164.
- (15) PDB deposition number: 3MVM.